



Climate change projections of rainfall and its impact on the cropland suitability for rice and wheat crops in the Sone river command, Bihar

Suraj Kumar¹ · Thendiyath Roshni¹ · Ercan Kahya² · Mohammad Ali Ghorbani²

Received: 28 November 2019 / Accepted: 6 July 2020 / Published online: 16 July 2020
© Springer-Verlag GmbH Austria, part of Springer Nature 2020

Abstract

Land suitability analysis is a necessity to achieve sustainable agricultural productivity with the optimum utilization of the available resources. Lack of proper knowledge on the best combination of factors that suit production of rice and wheat has contributed to low production in the Sone river command, Bihar. The aim of this study is to develop land suitability maps for rice and wheat crop based on physical, chemical and climatic factors of production using a multi-criteria evaluation (MCE) and Geographic Information System (GIS) approach. Biophysical variables of soil, climate and topography have been considered for suitability analysis. This work also evaluates the impact of climate change (CC) on cropland suitability for rice and wheat crops. Climatic variable scenarios of rainfall were obtained from four GCMs (CAN-ESM2, MPI-ESM-MR, CSIRO, CMCC-CMS) for three future time slices (2011–2040, 2041–2070, 2071–2100) of representative concentration pathways (RCP) RCP 2.6, RCP 4.5 and RCP 8.5 scenarios. The observation data (1985–2011) from IMD Pune from 8 meteorological stations were used as the current baseline climatic data of rainfall, which is used to validate the cropland suitability model. The results of CC indicate that there is a significant variability in the distribution of rainfall in the projected period 2011–2100 with respect to the baseline period. The results also show a concomitant increase in the projected crop suitability area of wheat from 17 to 35% and decrease in area for rice from 31 to 21% when compared with baseline for highly suitable area.

1 Introduction

Due to anthropogenic activities, the earth's climate system has experienced a lot of changes. The increase in extreme climatic events has already been detected as severity and frequency of the occurrence of drought, complex seasonal variation of rainfall and intense heat waves (US Climate

Change Science Program (USCCSP 2008)). Climate change (CC) has altered the hydrological process which results in uneven distribution of rainfall worldwide. Such change in rainfall patterns may keenly affect the productivity and phenology of growth and reproduction in arid and semiarid regions. The seasonal variability over many parts of arid and semiarid regions implies increasing uncertainty in the intensity of rainfall and its arrival time and duration of each rainfall event (Feng et al. 2013). India being an agricultural country is the main source of 17% of GDP (Jamil et al. 2018). The Sone command of Bihar state in India is one of the agriculturally prosperous regions, and the majority of the area is available for agricultural purposes (Kumar and Roshni 2019). Continuous land degradation and intense population growth towards the north of Sone command have put the land on enormous pressure. Demand of food increases and efficient agricultural productivity should be ensured and should be at par with the population increase (Johnson 1999; Rosegrant et al. 2001; FAO 2003; Patel and Markand 2014). Antecedent land suitability analysis is mandatory for agriculture sustainability (Bandyopadhyay et al. 2009;

✉ Thendiyath Roshni
roshni@nitp.ac.in

Suraj Kumar
suraj244263@gmail.com

Ercan Kahya
kahyae@itu.edu.tr

Mohammad Ali Ghorbani
ghorbani@tabrizu.ac.ir; m_ali_ghorbani@ymail.com

¹ National Institute of Technology Patna, Patna 800005, India

² Department of Civil Engineering, Istanbul Technical University, Istanbul, Turkey

Collins et al. 2001; Hopkins 1977). Hence, proper management of land resources is essential for agricultural sustainability.

To ensure food security, cropland suitability assessment becomes imperative to determine the appropriate type of crop in a region (Kurtener et al. 2004; Sarkar et al. 2014; Bonfante et al. 2018). Suitability of land depends on the requirement of crops and the features of the land (FAO 1976; Mustafa et al. 2011). There are many factors which need to be assessed for determining the suitability of the land (Belka 2005). Several studies on cropland suitability have been conducted worldwide (FAO 2007). Recent advances in GIS, Remote Sensing (RS) and Decision Support System (DSS) have allowed more precision in the field of agriculture specifically the cropland suitability (Akpoti et al. 2019). The investigation for land suitability employing GIS does not fully incorporate decision maker's preferences as it lacks a well-defined mechanism (Malczewski 2006). This problem can be solved by the integration of GIS with multi-criteria evaluation (MCE) methods. MCE is generally used as an effective tool for multi-criteria decision making. MCE integrated with GIS is useful, as variables can be evaluated and weights assigned depending on the importance of the parameters (Perveen et al. 2007). In the study of Kanlaya et al. (2009), the land suitability of sugarcane and cassava crops is achieved by the integration of multi-criteria decision making (MCDM) with FAO framework (1976). Mustafa et al. (2011) have integrated soil physical and chemical parameters using a multi-criteria decision making and GIS to generate cropland suitability for various crops. De La Rosa et al. (2004) have reviewed the analysis of qualitative and quantitative land evaluation methods and are compared by the methods of Manna et al. (2009). Their analysis suggests that to estimate the vulnerability, suitability of land, change in land use and management practices must be based on the results of land evaluation. A tool which enables the assessment of localised impacts of land related biophysical impacts has been developed by Duveiller et al. (2020). One of the key tools for ensuring sustainable agriculture and for attaining the current global food security goal in line with the Sustainability Development Goals (SDGs) of the United Nations is agricultural land suitability analysis (ALSA) (Akpoti et al. 2019).

The increase in the carbon dioxide and other greenhouse gases emissions are increasing due to population growth, industrialization and urbanization. Increase in greenhouse gases has altered the overall magnitude and seasonal distributions of rainfall in a greater extend (Feng et al. 2013). The extremity of rainfall due to the climate change has direct impact on agricultural production as timely sufficient rainfall is not available to the crops, where water availability and timing are the key factors for agricultural production. Soil texture changes very slowly and hence is not affected much due to climate change. Determination of soil pH is based on parent material,

vegetation, weathering rate and climate. Thus, it is not expected to change much due to climate change (Gelybó et al. 2018). Also, due to climate change, the organic carbon does not suffer much loss in carbon (Gottschalk et al. 2012).

Dell et al. (2014) investigated agricultural models that utilised rainfall, temperature and water as the factors for productivity. Rainfall forecasted using general circulation models, which have been used to analyse the impact of climate change on rainfall (Shashikanth and Sukumar 2017; Kumar et al. 2019a, b). Global climate models (GCMs) have been used widely for predicting future climate parameters (Tesfaye et al. 2017; Amanambu et al. 2019). Quantifying the effects of past and future cropland suitability helps the policy makers for adopting proper management measures and the selection of suitable crop species. A grid-based performance evaluation approach, as well as intercomparison framework to evaluate the uncertainty of climate models for rainfall production, has been proposed (Mehr and Kahya 2017).

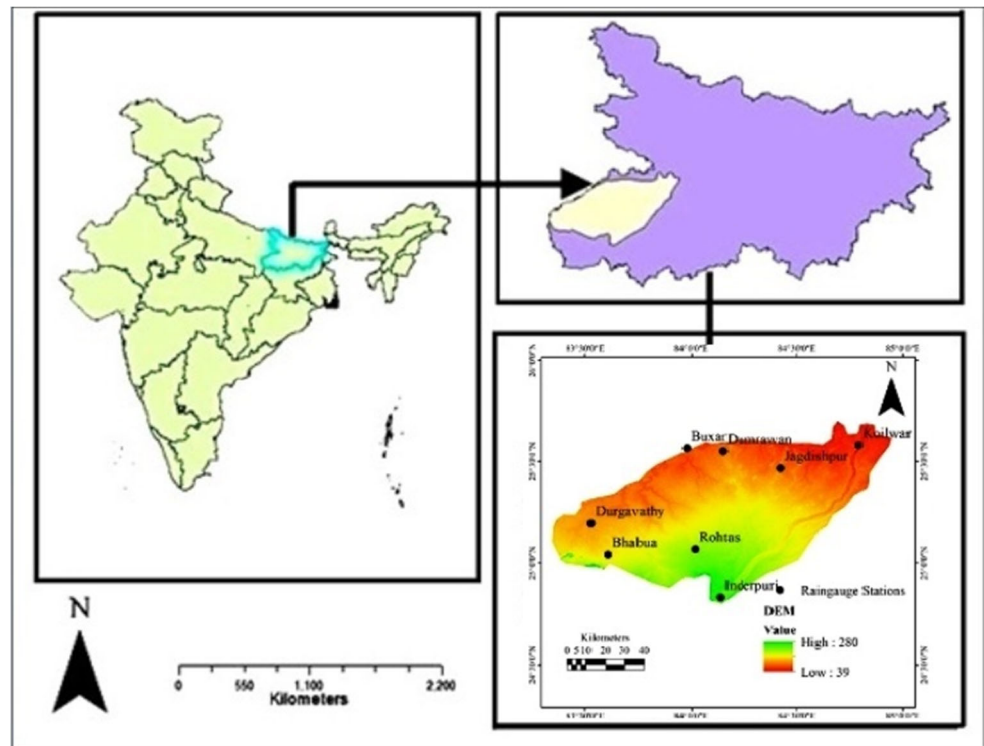
Accurate projection of rainfall is very important as the agricultural sector is immensely dependent on rainfall. Therefore, it becomes imperative to detect the cropland suitability analysis with spatio-temporal variation of rainfall, which is of utmost importance for the crop growth. Although several studies have focused on the MCE-GIS-integrated approach for crop suitability analysis, however to our knowledge, past literature work have not been reflected on the climate change impact on cropland suitability for agricultural crops. As Bihar is a major agricultural produce of rice and wheat crops, this work concentrates only on these two crops. The main purpose of the study is to develop the cropland suitability map of rice and wheat crops in view of the changing climatic conditions and to identify the area for expansion of the production of these crops. Cropland suitability for wheat and rice crops has been estimated for the period 2011–2100 and compared with the baseline period 1985–2011. The analytical hierarchy process (AHP) has been utilised for the multi-criteria evaluation for cropland suitability of rice and wheat crops. Four GCMs (CAN-ESM2, MPI-ESM-MR, CSIRO, CMCC-CMS) for three future time slices (2011–2040, 2041–2070, 2071–2100) of representative concentration pathways (RCP) RCP 2.6, RCP 4.5 and RCP 8.5 scenarios have been utilized for projecting rainfall.

2 Materials and methods

2.1 Study area and data acquisition

The study area covers the Sone command in Bihar, India (Fig. 1). It lies at latitude 24° 48' N and longitude 84° 07' E. The total command area of Sone command is 8600 km², which covers the districts Buxar, Bhojpur,

Fig. 1 Location of study area: Sone command in Bihar, India, and distribution of 8 rain gauge stations



Rohtas, Bhabua and Aurangabad. Soils are alluvial in nature and vary from light to heavy-textured clays in the top layer with coarse substrata (Kumar et al. 2019a, b). The plain alluvial soil is fertile and constitutes a wide spectrum of sand, silt and humus rich clay. Recent alluvium soil is found along the banks of river Ganga. The soil is medium to highly fertile. The command area selected is almost plain in topography and it uniformly slopes towards the Ganga river. All these aspects make the area ideal for irrigated agriculture. Rice is the main crop grown in the area in the Kharif (monsoon) season and wheat in Rabi season. Crops other than rice and wheat occupy less than 2% of the cultivable command area. The irrigation system has been operative since 1871; however, irrigation in an organized manner started in 1879 (Ahmad et al. 2015).

The input data used for the current study are slope map, soil pH, soil organic carbon content, rainfall and soil texture. The rainfall data of 8 stations Jagdishpur, Buxar, Inderpuri, Bhabua, Dumrawan, Durgavathy, Rohtas and Koilwar of the Sone River command for the period 1985–2011 have been used for cropland suitability analysis (Fig. 1). The observed rainfall data have been obtained from IMD Pune while the future rainfall data have been obtained from World Climate Research Programme (WCRP) CMIP5 model. The data used for model development and the source of data are detailed in Table 1. The area receives about 1100 mm of rainfall, over 80% of which occurs over the monsoon season (June to September) (Kumar and Roshni 2019).

2.2 Crop suitability analysis using AHP technique

Multi-criteria decision evaluation (MCDE) is a method designed to facilitate decision-making. The fundamental purpose is to consider a number of options in the light of various requirements and competing priorities. The primary issue in MCDE is concerned with how to combine the information from several criteria to form a single index of evaluation. The analytic hierarchy process (AHP), introduced by Saaty (1980), is one of the effective tools widely used for dealing with complex decision making, and may aid the decision makers to set priorities and make the best decision. In short, it is a method to derive ratio scales from paired comparisons.

2.2.1 Selection of parameters for crop suitability

The parameters that affect the crop suitability analysis are selected based on the past literature studies and suggestions from the experts (Ahamed et al. 2000, Worqlul et al. 2017). The parameters selected for the Sone river command are slope map, soil pH, soil organic carbon content, soil texture and rainfall. Crop development, suitability, nutrient availability and activity of microorganisms are affected by soil pH (USDA-NRCS 1998). High organic carbon is a symbol of good fertility conditions for crop production (FAO 1976). The productivity of crop is significantly affected by soil texture. The yield of rice is favourable in soil with higher water retention, while wheat requires soil with high oxygen content and better drainage. The spatial distribution of rainfall maps

Table 1 Description of the data used

Type of data	Description of data	Source of data
Rainfall data	1985–2011 2011–2100	IMD Pune https://esgf-node.llnl.gov/projects/cmip5/
Slope map	SRTM	USGS Earth Explorer(https://earthexplorer.usgs.gov/)
Soil pH, soil carbon content, soil clay content	Global gridded soil information	https://files.isric.org/soilgrids/data/recent/

has been made in ArcGIS 10.3 by importing the point rainfall data and then interpolating using IDW technique (Gong et al. 2014; Plouffe et al. 2015; Yang et al. 2015). The slope map has been generated by utilising the digital elevation model (DEM) of Shuttle Radar Topographic Mission (SRTM) having resolution of 90 m. A level surface favours equal distribution of water and is highly appropriate for rice cultivation (Samanta et al. 2011). The entire parameter maps have been georeferenced to UTM Zone 45 N in ArcGIS 10.3. The development of an adequate hierarchy structure is an ultimate objective for AHP (Fig. 2).

For calculating factor weights by comparing two factors together, pairwise comparison matrix introduced by Saaty (1980) is shown in Table 2. The scale varies from 9 to 1/9. A rating of 9 indicates that in relation to the column factor, the row factor is more important. On the other hand, a rating of 1/9 indicates that relative to the column factor, the row factor is less important (Kumar et al. 2016; Mustafa et al. 2011). A rating value of 1 is assigned in case the factors are equally

important. Based on the previous literature observations, a pairwise comparison matrix is prepared and utilised in this study for the weight generation and is shown in Table 4. In the diagonal, elements are assigned the value of unity. Priority vector is obtained by normalising principal Eigenvector. The priority vector is obtained by calculating the mean of the rows. The summation of all values of the priority vector is 1.

Consistency ratio (CR) is used to suggest the probability of random generation of matrix judgements (Malczewski 2006). The formulation of CR (is given in Eq. 1) in the AHP system is ratio between the consistency index (CI) of the matrix and the random index (RI) (Table 3) (Saaty 1980). The suitability levels of the parameters (Table 4) were finalised for CR values equal to or less than 10%. Table 5 details the normalised matrix.

$$CR = \frac{CI}{RI} \quad (1)$$

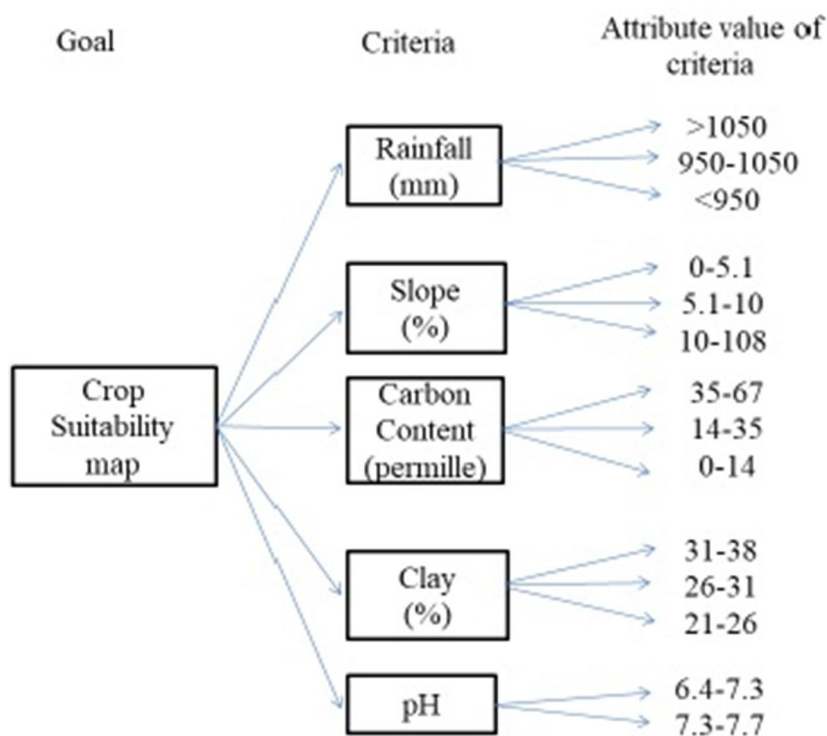
Fig. 2 Hierarchy for crop suitability

Table 2 The Saaty scale (2004) for pairwise comparison

Intensity of importance	Description
1	Equal importance
3	Moderate importance
5	Strong importance
7	Very strong importance
9	Extreme importance
2, 4, 6, 8	Intermediate values
Reciprocals	Values for inverse comparison

The CI refers to

$$CI = \frac{\lambda_{max} - n}{n - 1} \quad (2)$$

where n refers to the order of matrix and λ_{max} is the greatest Eigenvalue of preference matrix. In this study, the CR value of the matrix between 5 parameters is 0.0796 which is reasonable.

2.2.2 Standardization of criteria layers

Standardization is essential for suitability analysis as different parameters are measured in different units (Voodg 1983). The level of suitability for each parameter has been rated as highly suitable-S1, moderately suitable-S2, marginally suitable-S3, not suitable-N, based on the FAO 1976 guidelines for land suitability classification. All the parameters considered for suitability analysis have been reclassified using the guidelines for agricultural suitability by FAO (Table 6).

2.2.3 Weighted overlay analysis

The weights obtained by AHP process are assigned to the reclassified thematic maps of different variables. The weighted sum overlay of spatial analyst toolbox in ArcGIS 10.3 is then used for combining the different weighted maps (Eq. 3) to produce the final crop suitability map (S).

$$S = \sum_{i=0}^n (W_i * X_i) \quad (3)$$

where S is the final suitability, W_i is the weight of parameter i and X_i is the scale factor of parameter i .

The overall flowchart of the methodology that has been followed in this study is shown in Fig. 3.

Table 3 RI values

n	1	2	3	4	5	6	7	8	9	10
RI _s	0	0	0.58	0.9	1.12	1.24	1.32	1.41	1.45	1.49

Table 4 Suitability levels of the parameters used for AHP

Scale	Rainfall	Slope	Carbon content	Clay	pH
Precipitation	1	2	5	5	7
Slope	1/2	1	3	3	5
Carbon content	1/5	1/3	1	3	4
Clay	1/5	1/3	1/3	1	3
pH	1/7	1/5	1/4	1/3	1

2.2.4 Effects of climate change on rainfall

Effects of climate change on crops have been communicated a lot of times by several researchers and considered for modelling crop productivity (Tubiello and Ewert 2002). Four GCM models (Table 7) and their corresponding representative concentration pathways (RCP) RCP 2.6, RCP 4.5 and RCP 8.5 scenarios have been utilised in this study to project the rainfall for the period 2011–2100. As mentioned by Yan et al. (2015), rainfall simulation using GCMs exhibits good performance and relative independence. The projections have been carried out for 8 rainfall stations in the Sone river command. GCM data have various spatial resolutions. Hence, the data have to be brought to a common resolution for application. In this study, bilinear interpolation technique has been carried out to derive the rainfall data of the particular station for the projected period (2011–2100) located between midpoints of the four neighbour grids.

The climatic parameters obtained from GCMs are not always accurate. Bias correction is generally adopted method for developing relationship between the observed parameters and modelled parameters. In this paper, linear bias correction has been utilised (Eq. 4) for rainfall correction (Lenderink et al. 2007; Chen et al. 2013). This corrected rainfall data is utilised for further computations in this work.

$$P_{corrected} = P_{GCM} \times \frac{\mu(P_{observed})}{\mu(P_{GCM})} \quad (4)$$

where $P_{corrected}$ is the corrected annual rainfall, P_{GCM} is the annual rainfall obtained using GCM, $P_{observed}$ is the observed annual rainfall and μ is the mean of the rainfall data.

2.2.5 Mann-Kendall test

This test is frequently utilised to detect monotonic trend in weather data. The chance of detection of series as having a trend is more. The null hypothesis, H_0 denotes that the data are spread identically. Let x_1, x_2, \dots, x_n represent n data points where x_j represents the data point at time j . Then, the Mann-Kendall statistic (S) is defined as follows (Salas 1993)

Table 5 Normalised matrix of the parameters

	Rainfall	Slope	Carbon content	Clay	pH	Total	Priority Vector	Weight (%)
Rainfall	0.4895	0.5173	0.5218	0.4054	0.3500	2.2840	0.455	45.5
Slope	0.2448	0.2587	0.3131	0.2432	0.2500	1.3097	0.265	26.5
Carbon content	0.0979	0.0861	0.1044	0.2432	0.2000	0.7316	0.14	14
Clay	0.0979	0.0861	0.0347	0.0811	0.1500	0.4499	0.095	9.5
pH	0.0699	0.0517	0.0261	0.0270	0.0500	0.2248	0.045	4.5
Total	1	1	1	1	1	5	1	

$$S = \sum_{k=1}^{n-1} \sum_{j=k+1}^n \text{sgn}(x_j - x_k) \tag{5}$$

where the number of sample points is denoted by n , x_j and x_k which are the time-varying sample values where $j > k$ and assuming $x_j - x_k = \theta$, $\text{sgn}(\theta)$ is the sign function as,

$$\text{sgn}(\theta) = \begin{cases} +1 & \text{if } \theta > 0 \\ 0 & \text{if } \theta = 0 \\ -1 & \text{if } \theta < 0 \end{cases} \tag{6}$$

where a very high positive value of S denotes an increasing trend and a very low negative value denotes decreasing trend. P value is Mann-Kendall statistical parameter symbolizing the probability value. This value tests the hypothesis whether it is correct or not. If the hypothesis is wrong, the trend is significant and it is declined. P value < 0.05 signifies that there is trend and if Kendall’s tau value is positive, it signifies an increasing trend and if tau value is negative, the trend is decreasing. P value > 0.05 signifies that there is no monotonic trend. In this study, Mann-Kendall test has been carried out using XLSTAT 2018 which uses exact method for the calculation of p value.

2.2.6 Impact of climate change on cropland suitability

The water availability and timing are the key features for agricultural production. Studies have proven that climate change has altered the magnitude of rainfall and the seasonal distribution globally. Hence, it is important to analyse the change in precipitation pattern in the projected period for cropland suitability. The other parameters like soil texture and pH change

very slowly, and hence, the changes due to climate change are not considered in this study. The determination of soil pH is based on parent material, vegetation, weathering rate and climate. Thus, it is not expected to change much due to climate change (Gelybó et al. 2018). Also, due to climate change, the organic carbon does not suffer much loss in carbon (Gottschalk et al. 2012). Keeping these parameters like soil pH, carbon content, clay and slope of the area same, the cropland suitability maps for the future period have been generated utilising the projected rainfall obtained from the GCMs. The projected rainfall using GCMs (3 time slices i.e. 2011–2040, 2041–2070 and 2071–2100) is used for understanding the changes in a better way. The variation in the cropland suitability for rice and wheat has been examined with respect to the baseline period.

2.3 NDVI and LULC

NDVI stands for normalised difference vegetation index. It utilises multispectral remote sensing data to generate vegetation index. Near-infrared and red bands are the bands of satellite which are responsive to vegetation. The algorithm defined for calculating NDVI (shown in eq. 7) is the ratio of the difference of the red reflectance values from the near-infrared and the summation of near-infrared and red bands.

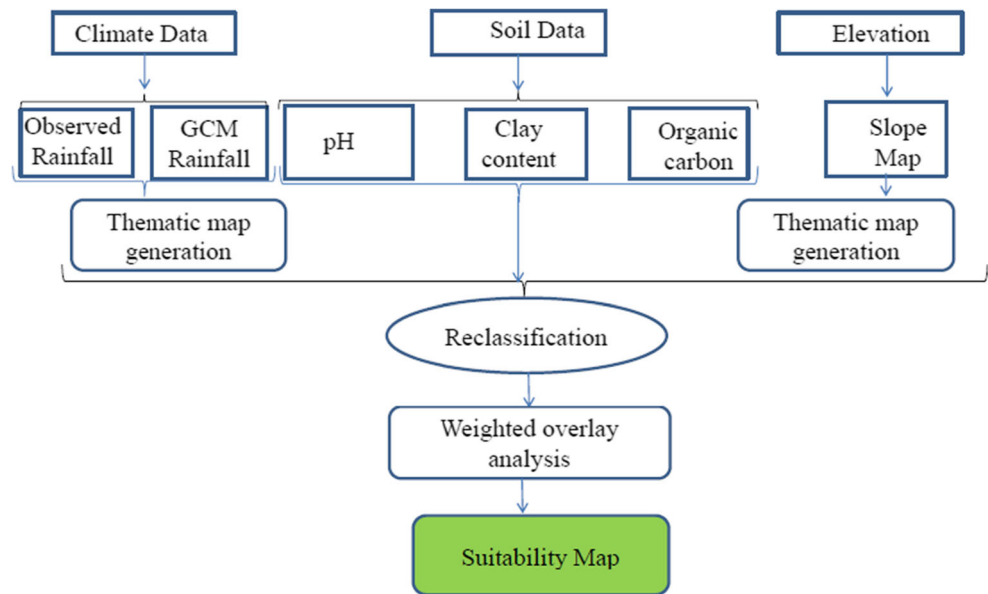
$$\text{NDVI} = (\text{NIR} - \text{RED}) / (\text{NIR} + \text{RED}) \tag{7}$$

where NIR and RED are the reflectance in the near-infrared and red region wavelengths respectively of the

Table 6 Parameters for crop suitability for rice and wheat

Parameter	Unit	S1		S2		S3	
		Rice	Wheat	Rice	Wheat	Rice	Wheat
Slope	%	0–5.1	0–5.1	5.1–10	5.1–10	10–108	10–108
Rainfall	Mm	> 1050	< 950	950–1050	950–1050	< 950	> 1050
Carbon content	Per mille	35–67	35–67	14–35	14–35	0–14	0–14
Clay	%	31–38	21–26	26–31	26–31	21–26	31–38
pH	pH	6.4–7.3	6.4–7.3	7.3–7.7	7.3–7.7		

Fig. 3 Outline of the methodology of cropland suitability



electromagnetic spectrum. The NDVI maps have been developed utilising OCM 2 filtered product downloaded from BHUVAN portal.

Landsat 8 satellite images (spatial resolution 30 m) have been obtained from Earth Explorer in the form of tiles (Table 8). Land use/land cover map for the year 2019 covering three classes water, built up and agriculture have been generated using supervised classification in ArcGIS 10.3.

3 Results and discussions

3.1 Cropland suitability analysis for rice and wheat crops for baseline (1985–2011)

As detailed in section 2.2, each layer feature for the cropland suitability has been analysed. The ability of each land feature has been assessed using symbols S1 (highly suitable), S2 (moderately suitable) and S3 (marginally suitable).

For the analysis, the slope map of the Sone river command is prepared and is shown in Fig. 4. Of the total area, 46.5% has very less slope of < 5.1% making the land highly suitable for the growth of crops. Moderately sloping 5.1–10% is 52.8% of the total area. Steeper terrain is 0.7% of the total area. The rice

crop cultivation is highly favoured in flat and level surfaces (Samanta et al. 2011).

The spatial distribution of the observed average rainfall for the baseline (1985–2011) is plotted and is shown in Fig. 5. It is seen that 10% of the area which lies in the upper part of the command area has received the average annual rainfall more than 1150 mm. Majority of the study area (77%) experienced average annual rainfall in the range 950–1150 mm thus making the study area suitable for the growth of crops like rice and wheat.

Using AHP technique, the weights of the selected parameters have been generated and are assigned to the reclassified maps of soil pH, carbon-content, slope, rainfall and clay content. The weighted maps are then overlaid in ArcGIS for generating the final cropland suitability maps of rice and wheat crops. The spatial distribution of the cropland suitability maps for rice and wheat crops of Sone river command and % suitability for different margins for the baseline is shown in Fig. 6. Rice crop requires high rainfall and suitable soil with high water retention properties. The crop suitability map shows that the regions of Rohtas and Koilwar districts are highly suitable for rice production. The marginally suitable part is unevenly spread across the whole basin. The high suitability is accounted for favourable soil properties, climatic conditions

Table 7 Details of the GCMs used for rainfall simulation for the period 2011–2100

Models	Scenario	Institution	Resolution
CAN-ESM2	RCP 2.6, RCP 4.5, RCP 8.5	Canadian Earth System Model	2.7906 × 2.8125
MPI-ESM-MR	RCP 2.6	Max Planck Institute for Meteorology (MPI-M)	1.8653 × 1.875
CSIRO	RCP 4.5	Commonwealth Scientific and Industrial Research Organisation, Australia	1.875 × 1.875
CMCC-CMS	RCP 4.5, RCP 8.5	Centro Euro-Mediterraneo per I Cambiamenti Climatici	3.7111 × 3.75

Table 8 Satellite data specifications

Satellite	Sensor	Path/row	Year of acquisition
Landsat 8	OLI	(141/042,141/043),(142/042, 142/043)	11/02/2019, 20/02/2019
Landsat 8	OLI	(141/042,141/043),(142/042, 142/043)	22/05/2019, 21/05/2019

and topography. The pie chart of the baseline period shows that 31% of the total area is highly suitable, 66% is moderately suitable and 3% is marginally suitable for rice crop. For wheat crop, the suitability map is predominantly of moderately suitable type. Highly suitable area is uneven for the baseline period covering the central part extending towards east and west. The pie chart of the suitability map of wheat symbolises that of the total area. The 17% area is highly suitable, 80% is moderately suitable and 3% area is marginally suitable for the crop production.

3.2 Impact of climate change on cropland suitability for rice and wheat crops

As mentioned, the rainfall is considered the only variable feature due to climate change in the present study. The rainfall data from four GCMs and three RCPs for the projected time period 2011–2100 has been selected and interpolated for the selected gauge sites. The whole data were segregated into three time slices (2011–2040, 2041–2070 and 2071–2100). The variation in rainfall as a result of changing climatic

conditions is illustrated in Table 9. The results reveal a very significant variation in rainfall for most of the GCMs when compared with the baseline.

For the time slice 2011–2040, all the models projected a decrease in rainfall with respect to baseline. CAN-ESM2 RCP 8.5 shows the highest decline of 14.33% while CAN-ESM2 RCP 2.6 shows the least decline. The period 2041–2070 also followed similar trend with all the stations showing a decline in rainfall from the baseline. CAN-ESM2 RCP 2.6 is displaying the highest decline of 14.537% while CSIRO RCP 4.5 is showing the least decline. For the period 2071–2100, 6 models are showing a decrease while the model CAN-ESM2 RCP 4.5 is showing a minor increase in rainfall. Overall, there is a decreasing trend in the average annual rainfall for most of the models from 2011 to 2100 in the Sone river command owing to the influence of climate change.

The rainfall is projected for all the selected gauge locations and the checked the bias corrections. To examine the spatio-temporal variation of the projected rainfall, the projected rainfall is plotted in Fig. 7. The changes in the projected rainfall

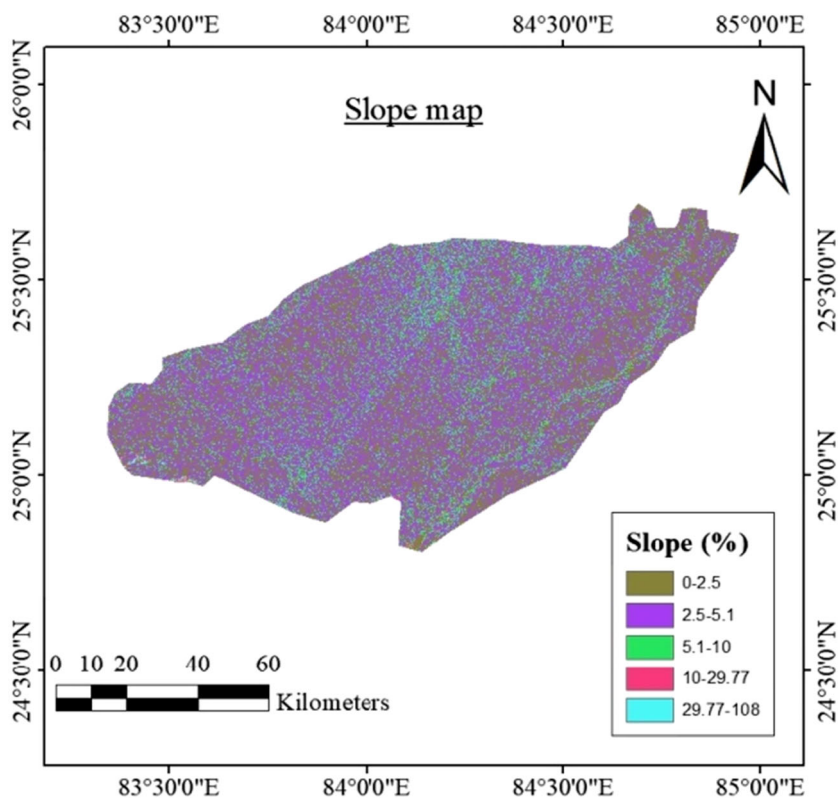
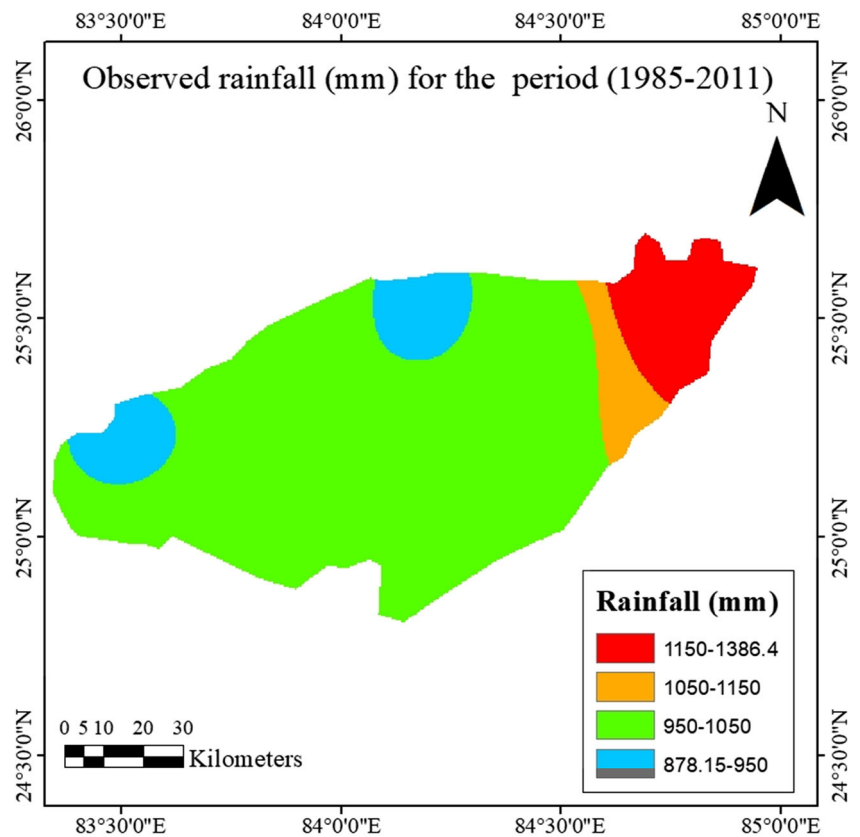
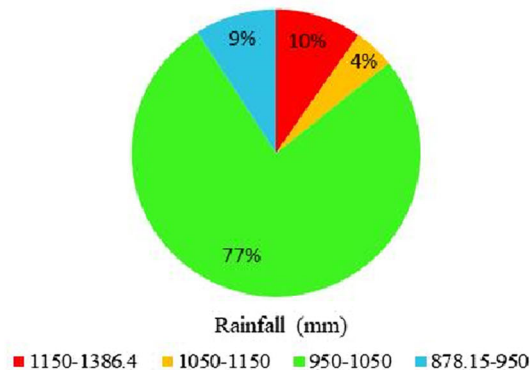
Fig. 4 A plot of slope map of the Sone river command

Fig. 5 Spatial distribution of average annual rainfall (mm) for the baseline 1985–2011 in Sone river command and the proportion of rainfall distribution in pie chart



Pie chart of rainfall distribution



are clearly visible in the figures for respective models and time slices. The rainfall obtained from the model CAN-ESM2 RCP 4.5 (2071–2100) shows the highest rainfall (> 1150 mm) spread of 11.4% of the total area and CAN-ESM2 RCP 8.5 (2011–2040) displayed the least area of 7.92% under rainfall > 1150 mm. Also, models CAN-ESM2 RCP 8.5, CSIRO RCP 4.5 (2011–2040) and CAN-ESM2 RCP 2.6 (2041–2070) display the highest area 47.44%, 44.95% and 48.55% respectively under the least rainfall of < 850 mm.

As the variations in the spatial distribution of rainfall are evident for each GCMs, the use of average downscaled values minimises the possible inhomogeneity or unrepresentativeness of station data (Wójcik 2015, Amanambu et al. 2019). In the present work also, as the differences of model results are very evident and hence, for each time slices, an average projected rainfall of all GCMs is calculated and is plotted in Fig. 8i. It is seen from figure that there are changes in the projected average rainfall with respect to the baseline. For

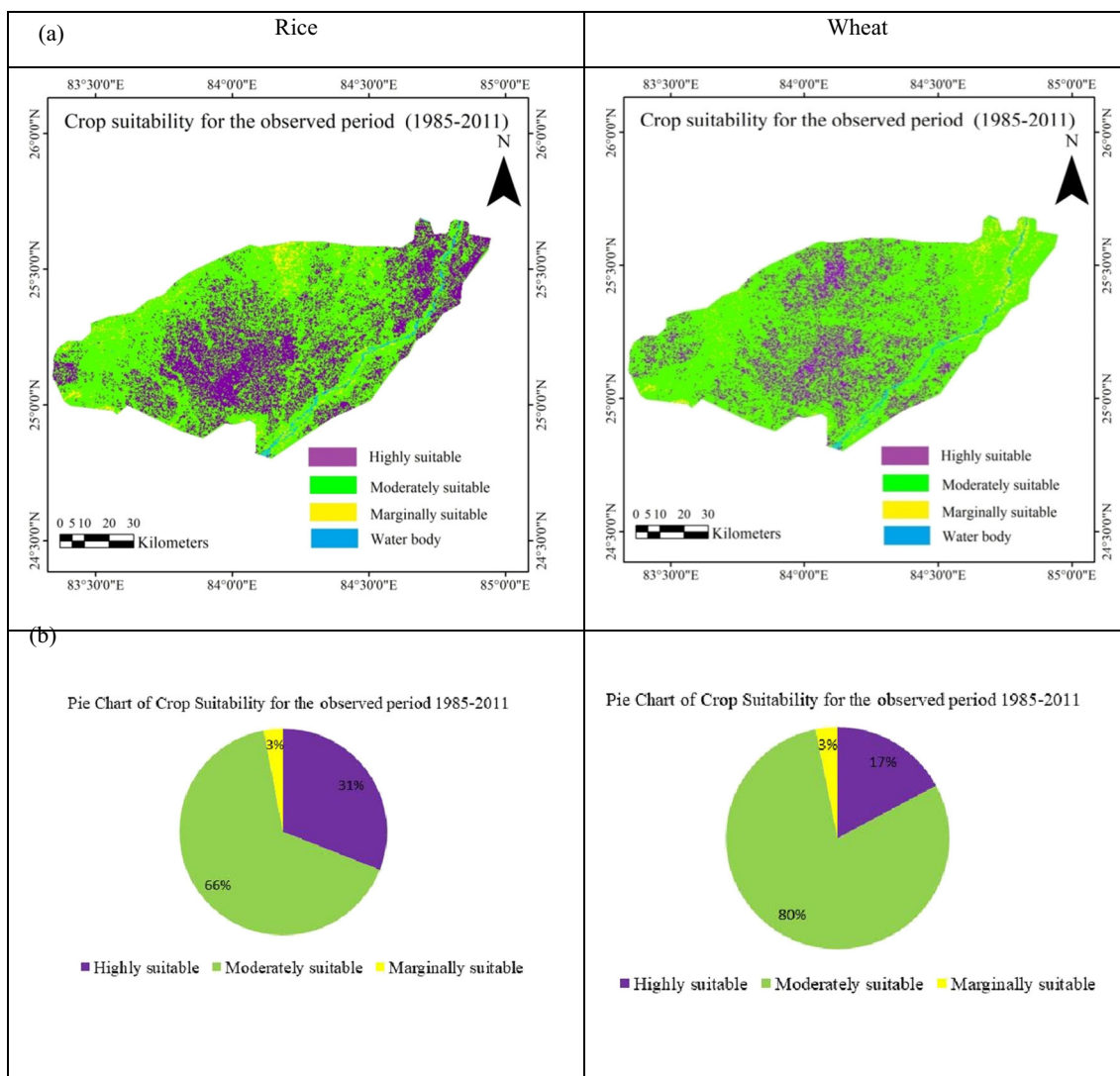
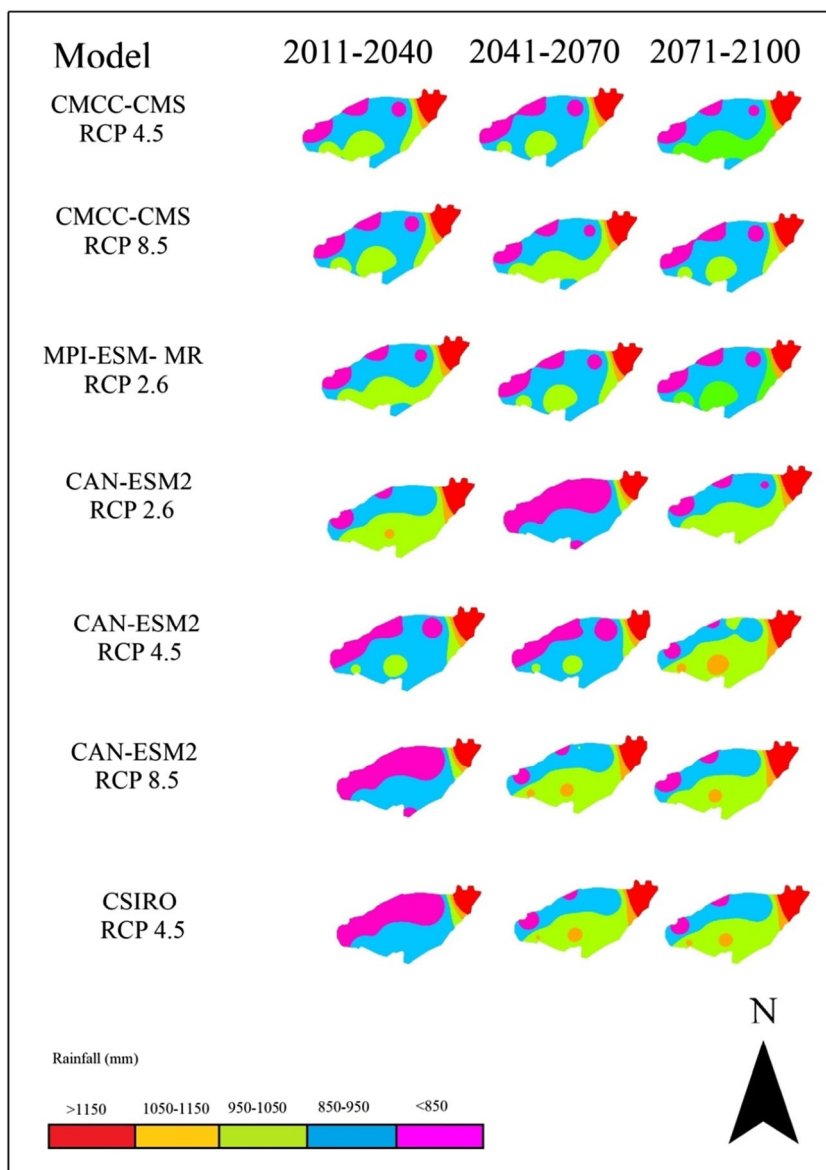


Fig. 6 a A plot of cropland suitability map for rice and wheat crop and b the distribution of area for highly, moderately and marginally suitable for rice and wheat crops in pie chart for the baseline (1985–2011)

Table 9 Changes in annual average projected rainfall (2011–2100) of different climate models with respect to the baseline

Climate models	Rainfall (mm) (2011–2040)	Change (%)	Rainfall (mm) (2041–2070)	Change (%)	Rainfall (mm) (2071–2100)	Change (%)
Baseline	1026		1026		1026	
CMCC-CMS RCP 4.5	955.97	− 6.82	946.91	− 7.707	968.49	− 5.60
CMCC-CMS RCP 8.5	955.39	− 6.88	967.77	− 5.674	947.87	− 7.61
MPI-ESM-MR RCP 2.6	966.26	− 5.82	952.20	− 7.192	952.70	− 7.14
CAN-ESM2 RCP 2.6	997.47	− 2.77	876.84	− 14.537	983.34	− 4.15
CAN-ESM2 RCP 4.5	932.86	− 9.07	924.27	− 9.915	1026.48	0.047
CAN-ESM2 RCP 8.5	878.89	− 14.33	1006.09	− 1.940	1004.90	− 2.055
CSIRO RCP 4.5	882.14	− 14.02	1009.14	− 1.643	1004.07	− 2.137
Average (GCMs)	938.43		954.74		983.98	

Fig. 7 Spatial distribution of the average annual rainfall for the projected time slices 2011–2040, 2041–2070 and 2071–2100



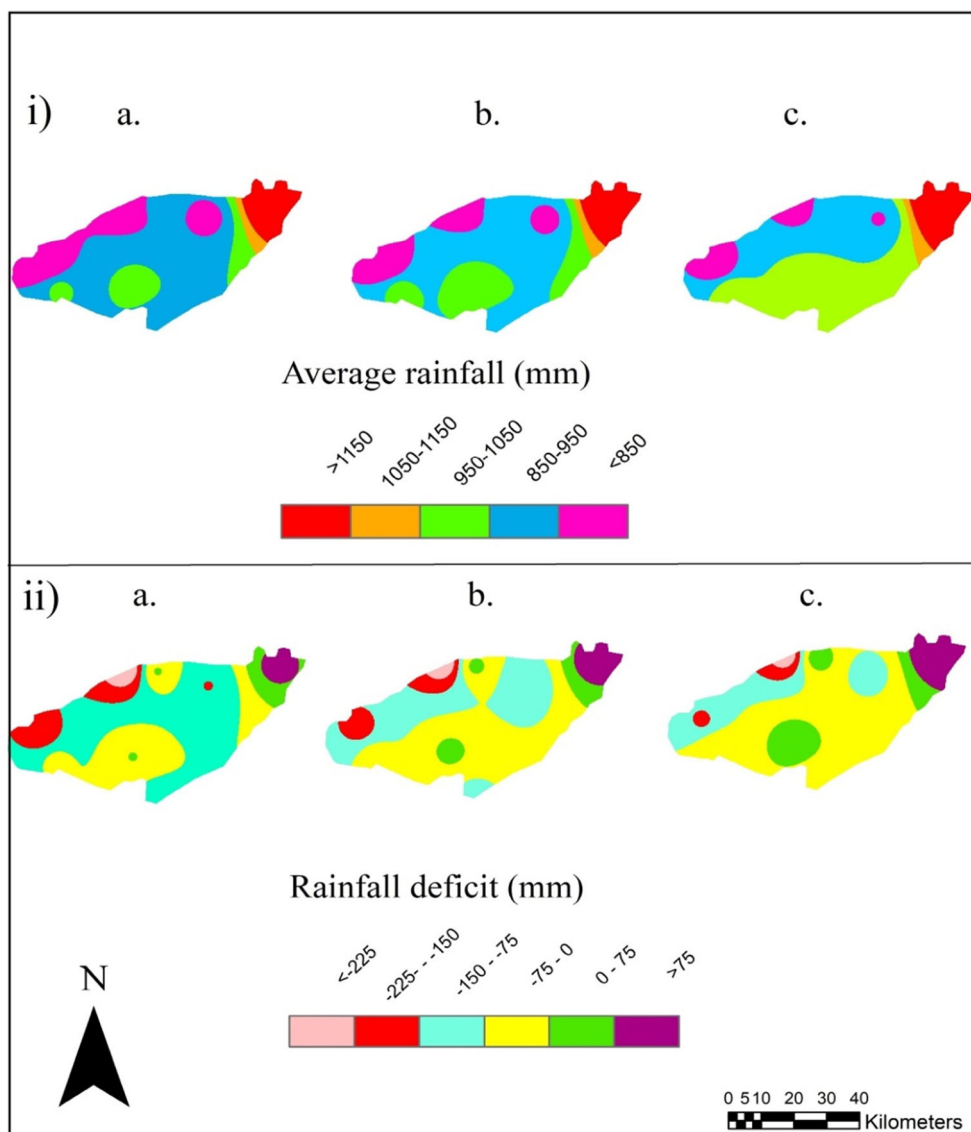
the period 2011–2040, 2041–2070 and 2071–2100, the rainfall at 5 stations Jagdishpur, Buxar, Inderpuri, Bhabua and Durgavathy is showing an increasing trend while at 3 stations Koilwar, Dumrawan and Rohtas, the rainfall is showing a declining trend. The current study also projected the rainfall deficit (Fig. 8ii), which is calculated as the difference in the future rainfall (which is the average of all the ensembles) with the base period and plotted for three time slices. For all the three time slices, rainfall deficit of <-225 mm is observed for the western part of the command with the highest area coverage of 1.04% for the time slice 2011–2040. The topmost part of the command is showing positive deficit or rainfall surplus of >75 mm for all the three time slices with the highest area of 7.7% for the time slice 2071–2100.

For understanding the pattern of the future rainfall trend analysis, using Mann-Kendall test has been carried out.

Trend analysis using Mann-Kendall test (Table 10) for the projected rainfall suggests that of the 8 stations, only 2 stations Dumrawan and Bhabua are showing increasing trend. No significant trend is observed for the rest of the stations.

Based on the projected rainfall data of different models, cropland suitability map for rice is generated and is plotted in Fig. 9 for the period 2011–2100. The results of crop suitability for different time slices fluctuated due to the non-uniform rainfall for different GCMs. It is observed that the suitability map of the study area differs with the GCMs and time. Highly suitable area for rice production is characterised by the central part and the northern part of the study area. The figure also depicts that the area with high rainfall has higher suitability for rice production. For the time slice 2011–2040, CSIRO RCP 4.5 is exhibiting the least area of 13% highly

Fig. 8 (i) Projected average rainfall (mm) and (ii) rainfall deficit for the period **a** 2011–2040, **b** 2041–2070 and **c** 2071–2100



suitable for rice crop, while CAN-ESM 2 RCP 2.6 is showing maximum area of 21% highly suitable for rice cultivation.

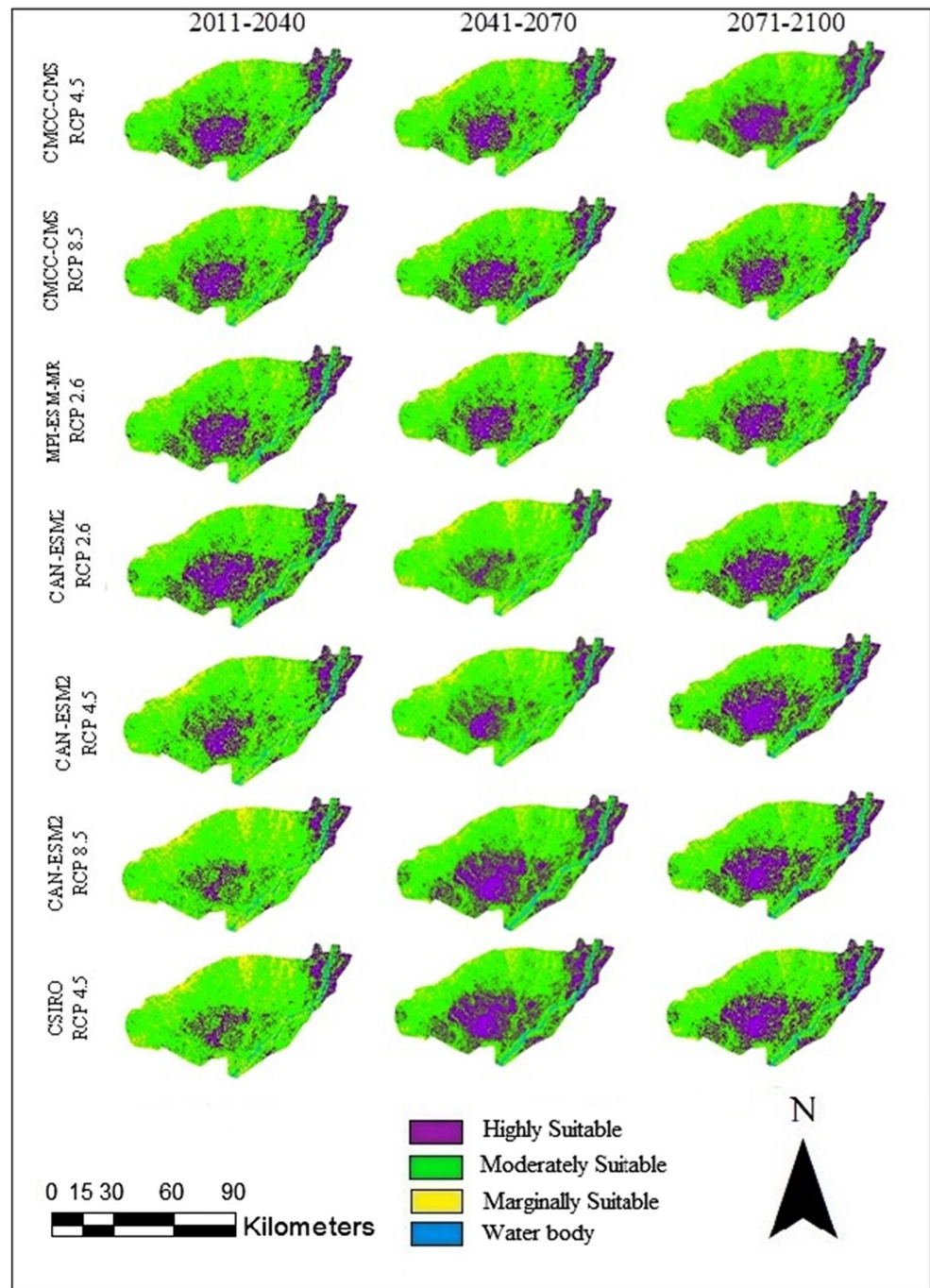
Table 10 Trend analysis of projected rainfall (2011–2100) of different stations employing average of GCM products

Station name	P value	Tau value	Trend
Jagdishpur	6.072383e-02	3.709009e-02	No trend
Durgavathy	5.081024e-02	3.862422e-02	No trend
Dumrawan	4.785805e-02	3.912943e-02	Increasing
Bhabua	4.994899e-02	3.876900e-02	Increasing
Buxar	5.572251e-02	3.783559e-02	No trend
Inderpuri	6.044601e-02	3.713014e-02	No trend
Koilwar	8.227486e-02	3.436378e-02	No trend
Rohtas	5.228589e-02	3.838085e-02	No trend

CAN-ESM 2 RCP 2.6 is showing least value of 10.5% and CAN-ESM 2 RCP 8.5 exhibits the highest area of 23% highly suitable for rice cultivation for the time slice 2041–2070. The period 2071–2100 projected an average area of 21% highly suitable for rice farming, which is high compared with the other two time slices. The results of MPI ESM MR RCP 2.6 show the least area of 19% while CAN ESM 2 RCP 4.5 is showing the highest area of 25% highly suitable for rice growth.

Figure 10 shows the projected average suitability map of rice crops for the periods 2011–2040, 2041–2070 and 2071–2100. It is seen that the land appropriate for rice production for the future time frame is evolving, which is ascribed to the rainfall which has indicated unevenness across the command. From the pie chart (Fig. 10), for the period 2011–2040, 19% area is most suitable, 72% area is moderately suitable and 9% area is marginally suitable.

Fig. 9 Spatial distribution of cropland suitability map of rice crop for the future time slices obtained from GCMs

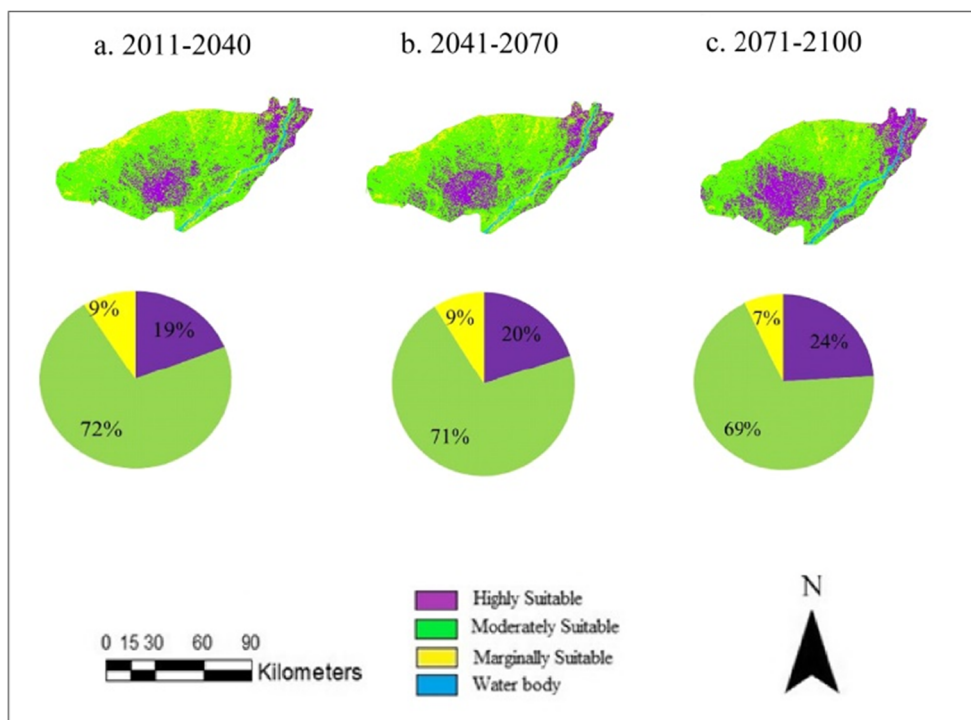


For the period 2041–2070, 20% is most suitable, 71% is moderately suitable and 9% is marginally suitable. The period 2071–2100 is showing higher value of most suitable area of 24%, 69% is moderately suitable and 7% is marginally suitable. Compared with the results of the observed cropland suitability, the average area of rice crop for the whole command will experience decrease in highly suitable area. During the period 2011–2040, the highly suitable area decreases by 38.7%, for the period 2041–2070, the area decreases by 35.5% and for the period

2071–2100, the decrease is 22.6% forming an overall decrease of highly suitable area from 31% to 21%.

The change in cropland area for rice crop suitability with respect to the baseline is shown in Fig. 11. Highly suitable area is decreasing for all the three time slices with the highest decrease of 12% for the period 2011–2040. Both moderately and marginally suitable areas experience an increase of 6%. For the time period 2041–2070, highly suitable cropland is showing a decrease of 11% while moderately suitable cropland is showing an increase of 5%. Marginally suitable area is

Fig. 10 Average of projected cropland suitability map for rice crop and pie chart showing the distribution of highly suitable, moderately suitable and marginally suitable for the period



showing an increase of 6%. The period 2071–2100 is showing a decrease of 7% for highly suitable cropland and an increase of 3% and 4% for moderately and marginally suitable cropland respectively.

Similarly, the cropland suitability map for wheat crop is also generated for the projected period 2011–2100 utilising 4 GCMs with 3 scenarios in Fig. 12.

The cropland suitability map using different scenarios is showing unevenness for wheat cultivation. Highly suitable area for wheat production is extending from the central part towards the southern part. The topmost part of the study area is moderately to marginally suitable for wheat production. For the period 2011–2040, CAN-ESM2 RCP 8.5 is showing maximum area 56.8% for highly suitable cropland for wheat, while CAN-ESM2 RCP 2.6 exhibits the lowest area highly

suitable for wheat production. Highly suitable area 56.93% is maximum for the model CAN-ESM2 RCP 2.6 while least 33.9% for CAN-ESM2 RCP 8.5. For the period 2071–2100, CSIRO RCP 4.5 is showing maximum highly suitable area of 56.4%, while the least area 35.8% is exhibited by CAN-ESM2 RCP 2.6.

Similarly, the cropland suitability map for wheat crop using average rainfall for the period 2011–2040, 2041–2070 and 2071–2100 is generated and shown in Fig. 13. The highly suitable area for wheat production is maximum for the period 2011–2040, while the period 2041–2100, the highly suitable area is decreasing. From the pie chart for the period 2011–2040, 40% of the total area is highly suitable, 58% is moderately suitable and 2% is marginally suitable. For the period 2041–2070, the highly suitable areas decrease to 36% and for

Fig. 11 Percentage changes in cropland suitability with respect to the baseline for rice crop

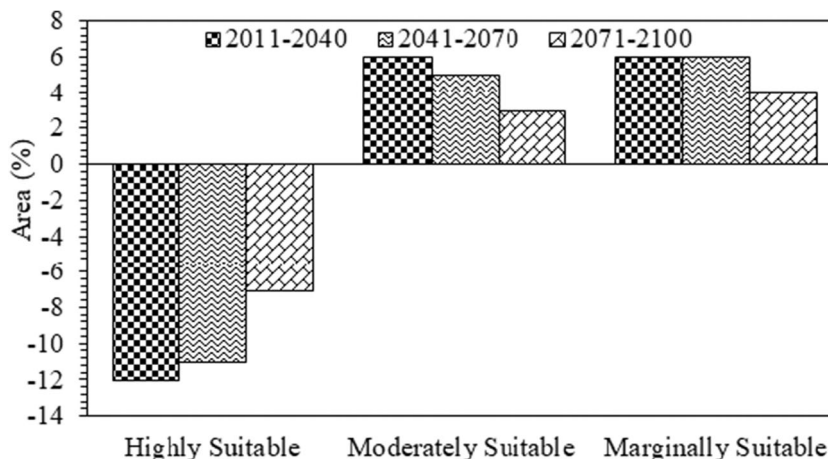
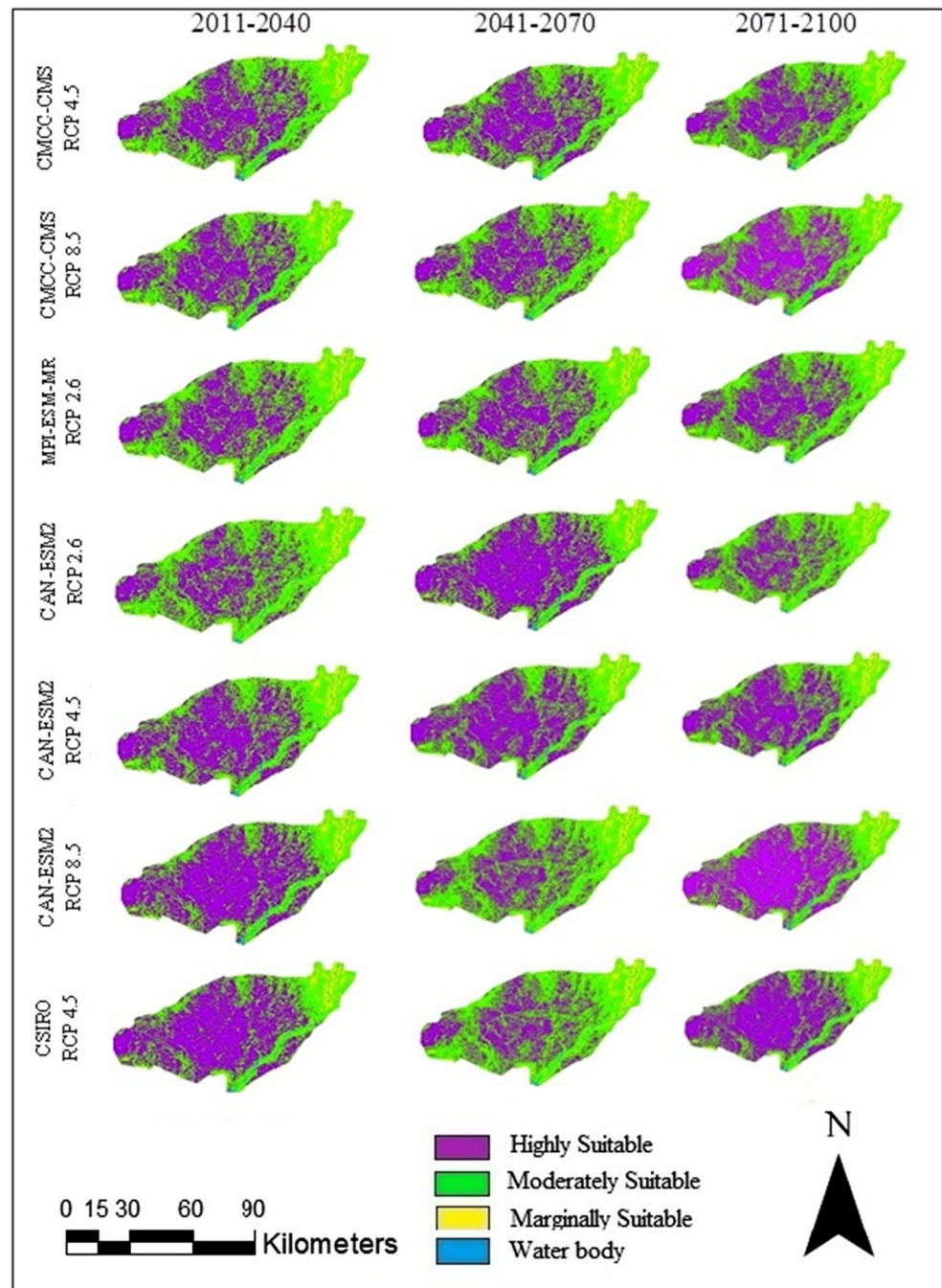


Fig. 12 Spatial distribution of cropland suitability map of wheat crop for the future period obtained from GCMs



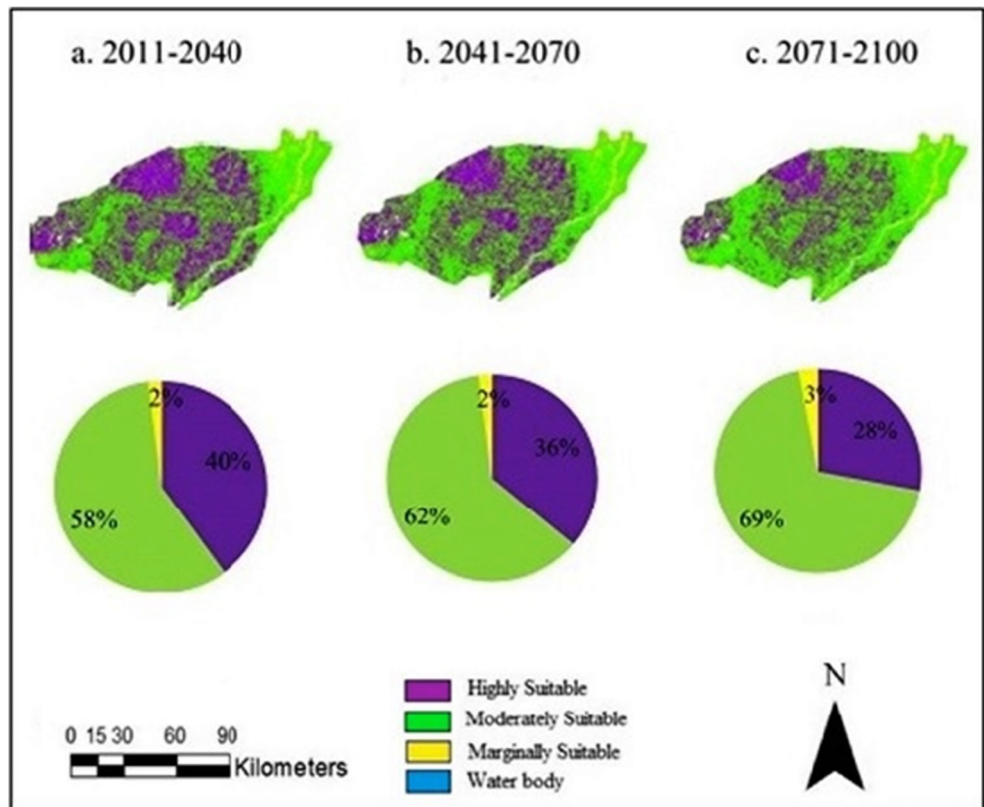
the period 2071–2100, the cropland again decreases to 28% (Fig. 13). The highly suitable area for wheat production during the baseline is 17% which increases to 34% by the end of 2070. For the wheat crop, there is an increase of cropland for highly suitable area from 17 to 35% during the period 2011–2100.

The change in cropland suitability of wheat with respect to the baseline has been shown in Fig. 14. For the time period 2011–2040, the highly suitable cropland has increased by 23% with respect to the baseline. The moderately and

marginally suitable cropland is displaying a decrease of 22% and 1% respectively. The 2041–2070 time period also exhibit an increase of 19% for highly suitable area while there is a decline of 18% and 1% for moderately and marginally suitable cropland respectively with respect to the baseline. For the period 2071–2100, there is an increase of 11% for highly suitable cropland and a decrease of 11% for moderately suitable cropland with respect to the baseline.

The LULC map (Fig. Fig.15) and NDVI map (16) have been compared with the generated cropland

Fig. 13 Average of projected cropland suitability map for wheat crop and pie chart showing the distribution of highly suitable, moderately suitable and marginally suitable for the period



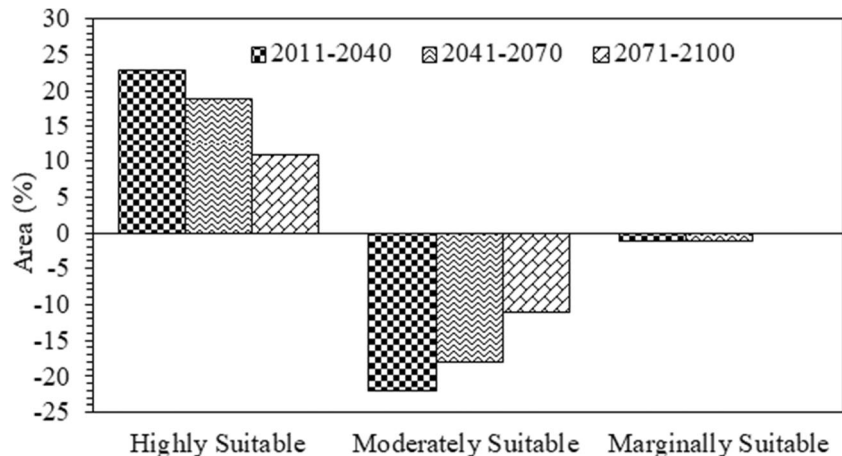
suitability map. It is seen that generated crop suitability map follows both the maps. The percentage area of vegetation is calculated from the NDVI maps and found that 97.5% area is showing proper vegetation in the month of February and 96.4% area in the September month for the year 2012 which is close to the projected average cropland suitable for the period 2011–2040 for rice which is 91% for rice and 98% for wheat. Also, the LULC map follows the cropland suitability map. Table 11 represents the distribution of the three LULC classes observed for

the year 2019 which demonstrates the accuracy of the crop suitability map.

4 Conclusions

Rice and wheat crops are the major food crops for majority of population across the world. Due to water shortage, improper soil and land properties, and ineffective farming practices, the yield of rice and wheat is decreasing. Therefore, it is

Fig. 14 Percentage changes in cropland suitability with respect to the baseline for wheat crop



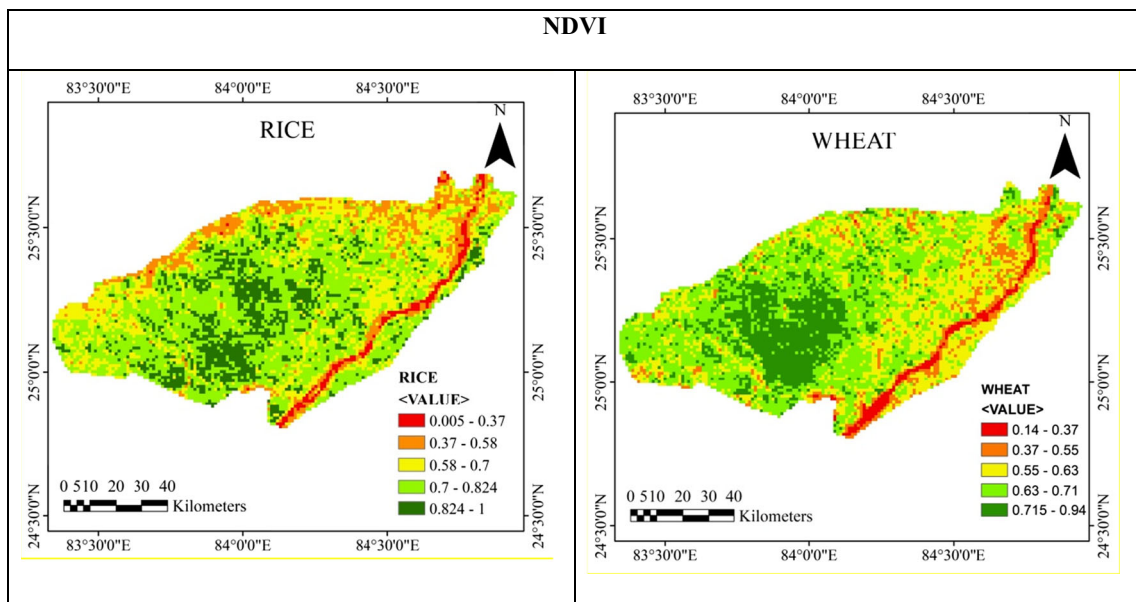


Fig. 15 NDVI for rice and wheat crops for the year 2012

imperative to distinguish the cropland suitability for the production of rice and wheat crops in the Sone river command. This study confirms the capability of integrated GIS and MCDA for generating long-term cropland suitability maps of the Sone river command. The cropland suitability maps are prepared using observed and GCMs climatic data of rainfall for the past (1985–2011) and future period (2011–2100). The rainfall is projected for four GCMs and three RCP scenarios. The average of the projected rainfall for the three time slices is used for the generation of cropland suitability maps for rice and wheat crops. The results of the projected rainfall

are showing an overall decreasing trend in the projected rainfall with respect to the baseline. Suitability analysis for the cropland suitability has been carried out using analytical hierarchical process for the two major crops rice and wheat. The study area has been divided into three classes i.e. highly suitable (S1), moderately suitable (S2) and marginally suitable (S3). The results signify that the largest area under highly suitable class is for wheat cultivation (35%) followed by rice cultivation (21%). These land features do not have any restrictions for crop cultivation. The projected cropland suitability signifies that most part of the study area is moderately suitable

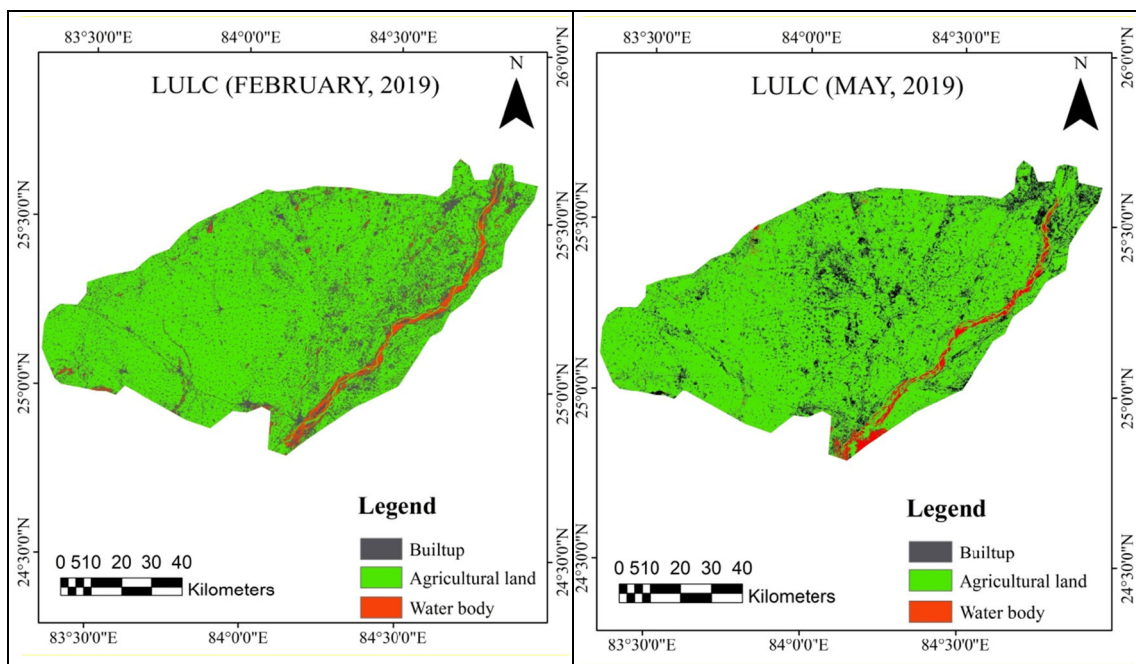


Fig. 16 LULC map of the Sone command for the year 2019

Table 11 Distribution of LULC (%)

	February (2019)	May (2019)
Built up/waste land	8.61	8.8
Agricultural land	89.39	87.24
Water body	2.84	3.96

for rice and wheat crops. Highly suitable area for rice experiences a decrease in crop area from 31 to 21%, while the area under wheat production shows an increase in area from 17 to 35% of the total area which suggests that wheat can be the key crop. The trend analysis using Mann-Kendall test shows that of the 8 stations, only 2 stations are showing an increasing trend while the rest of the stations show no trend. Rice cultivation is strongly influenced by water. Since only 2 stations are showing an increasing rainfall trend, it can be concluded that rice cultivation will show a decline while wheat which does not require much water experiences an increase. The cropland suitability map closely follows the NDVI map thereby asserting the authenticity of the developed maps.

Right place for the right crop is essential for the sustainable yields. Consequently, it is inferred that most of the study area has a huge potential for the production of cereal crops and can be brought under agriculture with varying degrees of suitability depending on future changes in climate. The result of this study is helpful for the farmers who are profoundly dependent on agriculture for the efficient cropland management and sustainable agriculture. For further research in this field, it is suggested that more factors like financial, social criteria and change in land use/land cover pattern ought to be chosen that will refine the accuracy of the result.

Acknowledgements The authors are grateful to Indian Meteorological Department (IMD), Pune, for the supply of climatic data used for carrying out this research work.

Compliance with ethical standards

Conflict of interest The authors declare that they have no known competing financial interests or personal relationships that could have appeared to influence the work reported in this paper.

References

- Ahamed TRN, Rao KG, Murthy JSR (2000) GIS-based fuzzy membership model for crop-land suitability analysis. *Agric Syst* 63(2):75–95
- Ahmad MM, Roy LB, Kumar A (2015) GIS based decision support system for efficient water management in Sone canal command area, *IJCSEIERD* 5(2): 43–56
- Akpoti K, Kabo-bah AT, Zwart SJ (2019) Agricultural land suitability analysis: state-of-the-art and outlooks for integration of climate change analysis. *Agric Syst* 173(C):172–208

- Amanambu AC, Li L, Egbinola CN, Obarein OA, Mupenzi C, Chen D (2019) Spatio-temporal variation in rainfall-runoff erosivity due to climate change in the Lower Niger Basin, West Africa. *CATENA* 172:324–334. <https://doi.org/10.1016/j.catena.2018.09.003>
- Bandyopadhyay S, Jaiswal RK, Hegde VS, Jayaraman V (2009) Assessment of land suitability potentials for agriculture using a remote sensing and GIS-based approach. *Int J Remote Sens* 30:879–895
- Belka KM (2005) Multicriteria analysis and GIS application in the selection of sustainable motorway corridor. Master's thesis submitted to linkopingsuniversitetInstitutionen for datavetenskap
- Bonfante A, Langella G, Mercogliano P, Bucchignani E, Manna P, Terribile F (2018) Science of the total environment a dynamic viticultural zoning to explore the resilience of terroir concept under climate change. *Sci Total Environ* 624:294–308. <https://doi.org/10.1016/j.scitotenv.2017.12.035>
- Chen J, Brissette FP, Chaumont D, Braun M (2013) Finding appropriate bias correction methods in downscaling precipitation for hydrologic impact studies over North America. *Water Resour Res* 49(7):4187–4205
- Collins MG, Steiner FR, Rushman MJ (2001) Land-use suitability analysis in the United States: historical development and promising technological achievements. *Environ Manag* 28:611–621
- De la Rosa D, Mayol F, Diaz-Pereira E, Fernandez M, De la Rosa Jr D (2004) A land evaluation decision support system (MicroLEIS DSS) for agricultural soil protection. With special reference to the Mediterranean region. *Environ Model Softw* 19:929–942
- Dell M, Jones BF, Olken BA (2014) What do we learn from the weather? *New Clim Econ Lit* 52(3):740–798. <https://doi.org/10.1257/jel.52.3.740>
- Duveiller G, Caporaso L, Abad-Viñas R, Perugini L, Grassi G, Arneith A, Cescatti A (2020) Local biophysical effects of land use and land cover change: towards an assessment tool for policy makers. *Land Use Policy* 91:104382
- FAO (1976) A framework for land evaluation, soil bulletin 32, FAO, Rome, 67
- FAO (2007) Land evaluation, towards a revised framework. Land and Water Discussion Paper 6. Rome: FAO Electronic publishing division
- FAO (2003). State of the World's Forests. Rome. <https://www.fao.org/docrep/fao/005/y7581e/>
- Feng X, DelSole T, Houser P (2013) Comparison of statistical estimates of potential seasonal predictability. *J Geophys Res-Atmos* 118: 6002–6016. <https://doi.org/10.1002/jgrd.50498>
- Gelybó G, Tóth E, Farkas C, Horel Á, Kása I, Bakacsi Z (2018) Potential impacts of climate change on soil properties. *Agrokém Talajt* 67(1): 121–141
- Gong G, Mattevada S, O'Bryant SE (2014) Comparison of the accuracy of kriging and IDW interpolations in estimating groundwater arsenic concentrations in Texas. *Environ Res* 130:59–69
- Gottschalk P, Smith JU, Wattenbach M, Bellarby J, Stehfest E, Arnell N, Osborn TJ, Jones C, Smith P (2012) How will organic carbon stocks in mineral soils evolve under future climate?: global projections using RothC for a range of climate change scenarios. *Biogeosciences*. 9(8):3151–3171 ISSN 1726-4170
- Hopkins LD (1977) Methods for generating land suitability maps: a comparative evaluation. *Journal of the American Institute of Planners* 43(4):386–400
- Jamil M, Sahana M, Sajjad H (2018) Crop suitability analysis in the Bijnor District, UP, using geospatial tools and fuzzy analytical hierarchy process. *Agric Res* 7(4):506–522. <https://doi.org/10.1007/s40003-018-0335-5>
- Johnson DG (1999) The growth of demand will limit output growth for food over the next quarter century. *PNAS* 96:5915–5920

- Kanlaya T, Songkot D, Chalie N (2009) Integration of land evaluation and the analytical hierarchical process method for energy crops in Kanchanaburi, Thailand. *Sci Asia* 35:170–177
- Kumar S, Roshni T (2019) NDVI-rainfall correlation and irrigation water requirement of different crops in the Sone river-command, Bihar. *MAUSAM* 70(2):339–346
- Kumar S, Roshni T, Pandey NG (2016) Spatial techniques in crop suitability analysis of Mahi sub-basin, proceedings of international conference on hydraulics, water resources and coastal engineering (Hydro2016), CWPRS Pune, India, 157–166
- Kumar K, Singh V, Roshni T (2019a) Efficacy of the hybrid neural networks in statistical downscaling of precipitation of the Bagmati River basin. *J Water Clim Chang*
- Kumar S, Roshni T, Himayoun D (2019b) A comparison of emotional neural network (ENN) and artificial neural network (ANN) approach for rainfall-runoff modelling. *C E J* 5: 2120–2130
- Kurtener D, Krueger-Shvetsova E, Dubitskaia I (2004) Quality estimation of data collection. UDMS. UDMS Press, Giorgia-Venice, pp 9101–9109
- Lenderink G, Buishand A, Van Deursen W (2007) Estimates of future discharges of the river Rhine using two scenario methodologies: direct versus delta approach. *Hydrol Earth Syst Sci* 11(3):1145–1159
- Malczewski J (2006) GIS-based multi-criteria decision analysis: a survey of the literature. *Int J Geogr Inform Sci* 20(7):703–726
- Manna P, Basile A, Bonfante A, De MR, Terribile F (2009) Comparative land evaluation approaches: an itinerary from FAO framework to simulation modelling. *Geoderma* 150(3):367–378. <https://doi.org/10.1016/j.geoderma.2009.02.020>
- Mehr AD, Kahya E (2017) Grid-based performance evaluation of GCM-RCM combinations for rainfall reproduction. *Theor Appl Climatol* 129(1–2):47–57
- Mustafa AA, Man S, Sahoo RN, Nayan A, Manoj K, Sarangi A, Mishra AK (2011) Land suitability analysis for different crops. A multi criteria decision making approach using remote sensing and GIS. Indian Agricultural Research Institute, New Delhi-110 012
- Patel JH, Markand PO (2014) Deriving crop calendar using NDVI time-series. *Int Arch Photogramm Remote Sens Spat Inf Sci* 40:869
- Perveen F, Ryota N, Intiaz U, Hossain KMD (2007) Crop land suitability analysis using a multicriteria evaluation and GIS approach, 5th international symposium on digital earth. The University of California, Berkeley, 1–8
- Plouffe CC, Robertson C, Chandrapala L (2015) Comparing interpolation techniques for monthly rainfall mapping using multiple evaluation criteria and auxiliary data sources: a case study of Sri Lanka. *Environ Model Softw* 67:57–71
- Rosegrant MW, Paisner MS, Meijer S, Witcover J (2001) Global food projections to 2020. Emerging trends and alternative future. International Food Policy Research Institute, Washington, DC
- Saaty TL (1980) The analytic hierarchy process. Planning, priority setting, resource allocation. McGraw Hill, New York, USA
- Saaty TL (2004) Decision making the analytic hierarchy and network processes (AHP/ANP). *J Syst Sci Syst Eng* 13:1, 35
- Salas JD (1993) Analysis and modeling of hydrologic time series. *Handbook of hydrology* 19:1–72
- Samanta S, Pal B, Pal DK (2011) Land suitability analysis for rice cultivation based on multi-criteria decision approach through GIS. *IJSET* 2 (1): 12–20
- Sarkar A, Ghosh A, Banik P (2014) Multi-criteria land evaluation for suitability analysis of wheat: a case study of a watershed in eastern plateau region, India, *Geo-Spat Inf Sci*, 17(2): 119–128. DOI: <https://doi.org/10.1080/10095020.2013.774106>
- Shashikanth K, Sukumar P (2017) Indian monsoon rainfall projections for future using GCM model outputs under climate change. *Adv Comput Sci Technol* 10(5):1501–1516
- Tesfaye K, Aggarwal PK, Mequanint F, Shirsath PB, Stirling CM, Khatri-Chhetri A, Rahut DB (2017) Climate variability and change in Bihar, India: challenges and opportunities for sustainable crop production. *Sustainability* 9:1998
- Tubiello FN, Ewert F (2002) Simulating the effects of elevated CO₂ on crops: approaches and applications for climate change. *Eur J Agron* 18:57–74
- U.S. Climate Change Science Program (USCCSP) (2008) Weather and climate ex-tremes in a changing climate, U.S. Climate Change Science, Program Synthesis Analysis Production 3.3 (<http://www.climatechange.gov/Library/sap/sap3-3/final-report/sap3-3-final-allpdf>)
- USDA (United States Department of Agriculture)-NRCS (National Resources Conservation Service) (1998) Soil quality information sheet. Soil Quality Institute, NRCS, USDA, and the National Soil Tilth Laboratory, GEO-SPATIAL INFORMATION SCIENCE 343 Agricultural Research Service, USDA. https://www.nrcs.usda.gov/Internet/FSE_DOCUMENTS/nrcs142p2_052208.pdf
- Voordt H (1983) Multicriteria evaluation for urban and regional planning. Pion, London
- Wójcik R (2015) Reliability of CMIP5 GCM simulations in reproducing atmospheric circulation over Europe and the North Atlantic: a statistical downscaling perspective. *Int J Climatol*, 35: 714–732. <https://doi.org/10.1002/joc.4015>
- Worqlul AW, Jaehak A, Dile YT, Osorio J, Schmitter P, Gerik T, Clark N (2017) Assessing potential land suitable for surface irrigation using groundwater in Ethiopia. *Appl Geogr* 85(1):1–13. <https://doi.org/10.1016/j.apgeog.2017.05.010>
- Yan D, Werners SE, Ludwig F, Huang HQ (2015) Hydrological response to climate change: the Pearl River, China under different RCP scenarios. *J Hydrol Reg Stud*, 4:228–245
- Yang X, Xie X, Liu DL, Ji F, Wang L (2015). Spatial interpolation of daily rainfall data for local climate impact assessment over greater Sydney region. *Adv Meteorol* 2015, 1, 12

Publisher's note Springer Nature remains neutral with regard to jurisdictional claims in published maps and institutional affiliations.